Temperature Dependence of Fusion and Fragmentation Kinetics of Triton X-100 Micelles

Yahya Rharbi,[†] Mei Li,[†] Mitchell A. Winnik,*[,†] and Kenneth G. Hahn, Jr.[‡]

Contribution from the Department of Chemistry, University of Toronto, 80 St. George St., Toronto, Ontario, Canada M5S 3H6, and ICI Paints Research Center, 16651 Sprague Road, Strongsville, Ohio 44136-1739

Received December 2, 1999. Revised Manuscript Received March 31, 2000

Abstract: This paper describes micelle exchange kinetics as a function of temperature for a pyrene derivative **1**, a triglyceride containing a pyrenebutyrate ester, solubilized in aqueous micelles of Triton X-100. The kinetics were followed by stopped-flow fluorescence time-scan measurements in which the disappearance of excimer over time was monitored. Two components of the exchange process could be separated: a first-order process with an activation energy of 110 kJ/mol, and a second process with an activation energy of 160 kJ/mol. Because the second-order process had a rate ($k_2 \approx 1 \times 10^6$ M^{-1} s^{-1}) at 24.6 °C that was nearly independent of the pyrene probe (**1**, 1-octylpyrene, 1-dodecylpyrene), the second-order process was assigned to a fusion-fragmentation mechanism, rather than a "sticky-collision" mechanism. The rates of the first-order process ($k_1 \approx 12$ s^{-1} for **1**) at 24.6 °C increased with decreasing size of the probe. This step was attributed to a fragmentation-growth mechanism in which the fragmentation rate is rate limiting. Exchange by this mechanism must involve fragmentation of a micelle containing two probe molecules to form two sub-micelles large enough to bear one of the probes.

Introduction

It is widely appreciated that when surfactants are dissolved in water, they self-assemble to form micelles if the surfactant concentration exceeds its critical micelle concentration. Most common surfactants form spherical micelles at low concentration, with aggregation numbers on the order of 60 to 100 molecules per micelle.[1] Micelles are able to solubilize organic solutes, enhancing the solubility in aqueous solution of substances with poor water solubility. One can use organic dyes as a means of estimating the cmc of the surfactant: As one adds surfactant to a solution, the cmc is taken to be the surfactant concentration where one observes a sudden increase in the solubility of the dye. Fluorescence quenching experiments, based upon the idea of a Poisson distribution of fluorescent dyes and quenchers among micelles, serve as the most common method for determining micelle aggregation numbers.[2]

For many years there has been a deep interest in the dynamics of micellar solutions. Many micellar systems have been examined by stopped flow, pressure jump, temperature jump, and ultrasonic relaxation measurements.[3] These measurements frequently identify two well-separated relaxation times, a rapid relaxation that occurs on a time scale of microseconds and a slower process, which requires milliseconds to seconds.[2−4] Aniansson and Wall[5,6] assigned the fast process to an association−dissociation process involving the exchange of individual surfactant molecules between the micelles and the water phase, and attributed the slower process to a more deep-seated rearrangement of the system involving the creation or destruction of micelles. A cartoon describing these two processes is presented in Chart 1. Aniansson et al.[6] have shown that one can calculate the exit (k^-) and re-entry (k^+) rate constants for the surfactant molecules from the concentration dependence of the fast relaxation time. For the nonionic surfactant Triton X-100,[7] which we examine in this paper, they found $k^- = 1.1 \times 10^6$ s^{-1} and $k^+ = 3.7 \times 10^9$ M^{-1} s^{-1} at 25 °C.

The molecular process associated with k^- is identified by the strong decrease in the exit rate as the number of CH_2 groups in the surfactant is increased. Identifying the slow process is more difficult. The most compelling experiments are those in which surfactant solution above the cmc is rapidly diluted below its cmc. The time scale for this process (seconds) corresponds to that found by the other methods mentioned above. As we will see below, there are other slow dynamic processes of micelles that have proved exceptionally difficult to study directly. These include second-order processes involving the collision of two micelles and the first-order fragmentation of a micelle into a pair of smaller aggregates.

[†] University of Toronto.

[‡] ICI Paints Research Center.

(1) Israelachvili, J. *Intermolecular and Surface Forces*; Academic Press: London, 1992.

(2) Zana, R. In *Surfactant Solutions*: *New Method of Investigation*; Zana, R., Ed.; Marcel Dekker: New York, 1987.

(3) For reviews of dynamic processes in micelles, see: (a) Muller, N. In *Solution Chemistry of Surfactants*; Mittal, K. L., Ed.; Plenum: New York, 1979; Vol. I, pp 267−295. (b) Gormally, J.; Gettins, W. J.; Wyn-Jones, E. In *Molecular Interactions*; Wiley: New York, 1980; Vol. 2, pp 143−177. (c) Lang, J.; Zana, R. In *Surfactant Solutions*: *New Methods of Investigation*; Zana, R., Ed.; Marcel Dekker: New York, 1987; pp 405−452. (d) Huibers, P. D. T.; Oh, S. G.; Shah, D. O. In *Surfactants in Solution*; Chattopadhay, A. K., Mittal, K. L., Eds.; Marcel Dekker: New York, 1995; Vol. 64, pp 105−121.

(4) Lang, J.; Tondre, C.; Zana, R.; Bauer, H.; Hoffmann, H.; Ulbricht, W. *J. Phys. Chem.* **1975**, *79*, 275.

(5) Aniansson, E. A. G.; Wall, S. N. *J. Phys. Chem.* **1974**, *78*, 1024−1030. Aniansson, E. A. G.; Wall, S. N. *J. Phys. Chem.* **1975**, *75*, 857.

(6) Aniansson, E. A. G.; Wall, S. N.; Almgren, M.; Hoffmann, H.; Kielmann, H.; Ulbricht, W.; Zana, R.; Lang, J.; Tondre, C. *J. Phys. Chem.* **1976**, *80*, 905.

(7) Hoffmann, H.; Kielmann, H.; Pavlovic, D.; Platz, G.; Ulbricht, W. *J. Colloid. Interface Sci.* **1981**, *80*, 237.

10.1021/ja9942585 CCC: $19.00
Published on Web 06/17/2000

Chart 1

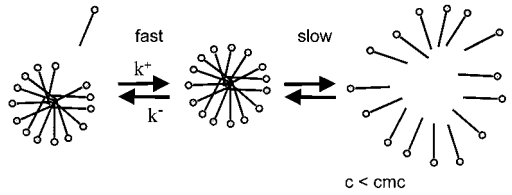

When the micelles contain hydrophobic solutes, another type of dynamics becomes important: the exchange of solute molecules between micelles.[2,8,9] As in the case of surfactant exchange, the dominant mechanism is an "evaporation−condensation" process involving passage of individual solute molecules through the water phase. When the solute is a luminescent dye or a quencher of the fluorescence or phosphorescence of a dye localized in the micelles, time-resolved luminescence quenching experiments can be used to determine the exit and entry rates of the solute from and into the micelles.[2,10−12] One finds that the exit rates are rate limiting, whereas the entry rates are close to diffusion controlled. Within a series of solutes containing a different number of aromatic rings or different alkyl substituents, the exit rate decreases rapidly with decreasing water solubility.[2,9] Fluorescence quenching experiments[8,9] are sensitive to fast exchange rates, whereas triplet-quenching measurements,[10−16] because of the longer-lived excited state, are sensitive to slower exit rates.

Oil−water−surfactant microemulsions have many features in common with surfactant micelles. Both contain a dispersed state consisting of domains of nanometer dimensions, and both represent a thermodynamically stable state of their respective systems. One of the important differences is that in microemulsions, the dispersed state is not dilute. Another difference is that the surface tension between the two phases in a microemulsions is very small. Microemulsions are employed in a broad spectrum of applications such as encapsulation, cosmetics, and printing.[17] As a consequence, there is a deep interest in learning how to control the structure, stability, and dynamics of microemulsion compositions. A major issue is the kinetics of oil exchange between droplets in microemulsions.

For oil-in-water microemulsions, the oil exchange process is conceptually similar to the solute exchange process between spherical aqueous micelles. Solutes and surfactant in both types of systems can exchange via various mechanisms. One mechanism involves the exit of individual solute or surfactant molecules into the aqueous phase followed by entry into another droplet. This exit−reentry mechanism is important for all species that have a sufficient solubility in water. In the second mechanism, there is a sequence of events involving the collision of two micelles, the exchange of their contents, followed by their separation. The first step is analogous to the fusion process observed for single lamellar vesicles in solution.[18] The collision−exchange−separation process has been suggested as a mechanism to explain rapid exchange in microemulsions as well as in nonionic surfactant micelles at high concentrations or at elevated temperatures. The third mechanism involves fragmentation of a micelle into two smaller entities often referred to as "sub-micelles" followed by their growth into normal micelles.

Chart 2

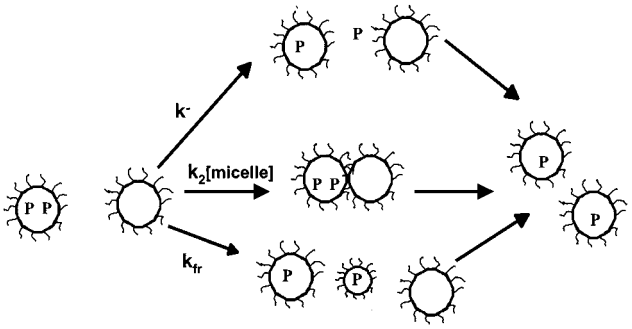

We depict these three different solute exchange mechanisms in Chart 2. The circles refer to the micelle core, and letter P's refer to the solute. While this diagram is general for any spherical surfactant micelles, we are in this paper particularly interested in pyrene derivatives (P) solubilized by Triton X-100, a nonionic surfactant. We draw wiggly lines at the edge of the circles in Chart 2 to refer to the flexible oligo(ethylene oxide) chains at the surface of nonionic surfactant micelles.

Zana et al.[19] studied the kinetics of pyrene excimer formation in several nonionic surfactant micelles at temperatures close to the cloud point. They analyzed their data using a model that incorporated pyrene exchange among micelles as an important step in the excimer-forming reaction, and inferred that a fusion−fragmentation exchange takes place in some of the systems. In these experiments, the solubility of pyrene in water, although small (7×10^{-7} M at 23 °C), is still large enough that exit−reentry kinetics competes with the micelle fusion−fragmentation exchange.

The mechanism involving fragmentation of micelles has been suggested to explain solute exchange in ionic surfactant micelles at high ionic strength. This type of mechanism was proposed by Malliaris et al.[20] to explain the fast exchange of pyrene among dodecylammonium chloride micelles at various salt concentrations. Both Almgren et al.[21] and Bohne and Scaiano[22] have reported examples of exchange processes with rates independent of the empty micelle concentration. Bohne and Scaiano observed a slow exchange of dodecylpyrene (C_{12}Py) between sodium dodecyl sulfate (SDS) micelles in water. They concluded that the exchange occurs via a process similar to the fragmentation−growth mechanism. Despite the progress in developing reasonable exchange mechanisms and using them to explain experimental observations, designing experiments to measure micelle exchange rates directly for each of these mechanisms remains a challenge.

In this paper we begin with the hypothesis that if one selects a pyrene derivative with a negligible solubility in water, then only the collision−exchange−separation and fragmentation−separation mechanisms will lead to exchange of solutes between micelles. We take advantage of the difference in the kinetics of these two mechanisms to separate their contribution

(8) Barzykin, AV.; Tachiya, M. *Heterog. Chem. Rev.* **1996**, 3, 105.
(9) Gehlen M. H.; De Schryver F. C. *Chem. Rev.* **1993**, *93*, 199.
(10) Infelta, P. P.; Grätzel, M.; Thomas, J. K. *J. Phys. Chem.* **1974**, *78*, 190.
(11) Bolt, J. D.; Turro, N. J. *J. Phys. Chem.* **1981**, *85*, 4029.
(12) Almgren, M.; Grieser, F.; Thomas, J. K. *J. Am. Chem. Soc.* **1979**, *101*, 2021.
(13) Scaiano, J. C.; Selwyn, J. C. *Can. J. Chem.* **1981**, *59*, 2368.
(14) Selwyn, J. C.; Scaiano, J. C. *Can. J. Chem.* **1981**, *59*, 663.
(15) Pileni, M. P.; Grätzel, M. *J. Phys. Chem.* **1980**, *84*, 1822.
(16) Hruska, Z.; Piton, M.; Yekta, A.; Duhamel, J.; Winnik, M. A.; Riess, G.; Croucher, M. D. *Macromolecules* **1993**, *26*, 1825.
(17) (a) Taisne, L.; Cabane, B. *Langmuir* **1998**, *14*, 4744. (b) Almgren, M.; Stam, J. V.; Swarup, S.; Löfroth, J. E. *Langmuir* **1986**, *2*, 432.
(18) Duzgunes, N.; Allen, T. M.; Fedor, J.; Papahadjopoulos, D. *Biochemistry* **1987**, *26*, 8435.
(19) Zana, R.; Weill, C., *J. Phys. Lett.* **1985**, *46*, 953.
(20) Malliaris, A.; Lang, J.; Zana, R. *J. Phys. Chem.* **1986**, *90*, 655.
(21) Almgren, M. *Chem. Phys. Lett.* **1980**, *71*, 539.
(22) Bohne, C.; Konuk, R.; Scaiano, J. C. *Chem. Phys. Lett.* **1988**, *152*, 156.

to the exchange process. We employ the pyrene-substituted triglyceride **1** as a solute to study exchange in Triton X-100 (TX-100) micelles in dilute solution in water at various temperature ranging from 5.3 to 24.6 °C. Solutions can be prepared in which some micelles contain more than one molecule of **1**. The fluorescence spectra of these solutions are characterized by a strong excimer emission. When one of these solutions is mixed under stopped-flow conditions with an excess of empty micelles, exchange takes place. One can follow this process in a time-scan experiment by monitoring either the growth in intensity of the blue "monomer" emission (I_M) or the decrease in excimer intensity (I_E).

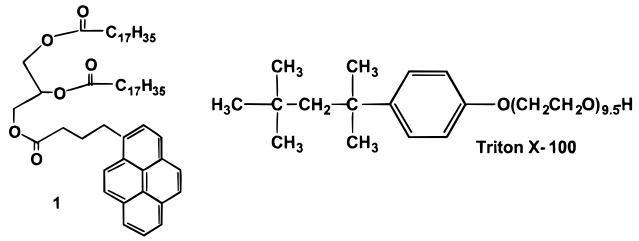

The collision−exchange−separation process follows second-order kinetics. The rate of this process is first order in the concentration of empty micelles. The fragmentation−growth mechanism follows first-order kinetics with a rate independent of the concentration of empty micelles. We show that both processes operate in the exchange of solute in nonionic surfactant Triton X-100 micelles. For example, the rate constant for the fragmentation−growth process for **1** is 12 s^{-1} at 24.6 °C. We establish that the second-order process is reaction-controlled rather than diffusion-controlled, with a second-order rate constant $k_2 = 1.3 \times 10^6$ M^{-1} s^{-1} at 24.6 °C. Because the rate of this step is nearly independent of the solute, we infer that the fusion step is rate limiting in the exchange process.

Experimental Section

Materials. The molecule **1** ($M_w = 882$) is a triglyceride in which 4-(1-pyrene)butyric acid is one of the constituent fatty acid esters. Its synthesis and characterization is described elsewhere.[23] Triton-X 100 (TX-100, Aldrich, manufactured by Union Carbide) is an octylphenol ethoxylate with an average of 9.5 ethylene oxide (EO) groups per molecule that was used as received. Distilled water was further purified through a Millipore Milli-Q purification system.

Surfactant Solutions Containing 1. A solution of Triton X-100 (21.66 g/L) was mixed with 0.1 mg of **1**. The mixture was heated at 75 °C (above the melting point of **1**) and strongly agitated for 15 min with a Vortex Genie 2, model G 560, mechanical shaker at its maximum frequency (>10 Hz). The solution was then allowed to cool to room temperature over 2 h, and then filtered through a 0.2 μm filter to remove a tiny amount of solid. This transparent solution was diluted with aqueous surfactant solution and then with water to yield a solution containing 0.68 mM TX-100 and 2.15 μM **1**. For TX-100, with an aggregation number of 100, this solution has a mean occupancy number $\langle n \rangle$ of 0.44 molecules of **1** per surfactant micelle.[23]

The amount of **1** solubilized in each TX-100 solution was determined by UV spectroscopy using the value $\epsilon_{346} = 4.7 \times 10^4$ M^{-1} cm^{-1} determined previously.[23] Absorption spectra of **1** were measured with a Hewlett-Packard 8452A diode-array spectrometer, using a 1.00 cm cell. The background was subtracted using a TX-100 solution of the same concentration as a reference. The absorbance of **1** was calculated relative to that at 398 nm, which was considered as the baseline.

Fluorescence Measurements. Steady-state and time-scan fluorescence measurements were carried out with a SPEX (2.1.2) Fluorolog spectrometer in the S/R mode. The intensity was kept below 2×10^6 counts/s to maintain the linearity of the detector response, which was calibrated prior to running these experiments. For emission spectra and for time-scan kinetics experiments, $\lambda_{ex} = 346$ nm, whereas excitation spectra were obtained for both $\lambda_{em} = 375$ nm (monomer) and $\lambda_{em} = 480$ nm (excimer). Fluorescence decay profiles of excited pyrene were measured by the single-photon-timing technique with $\lambda_{ex} = 346$ nm and $\lambda_{em} = 375$ nm. The excitation source was a coaxial flash lamp (Edinburgh instrument model 199 F) filled with deuterium.

Exchange Kinetics Experiments. In the measurements of exchange kinetics, the samples were mixed in the sample chamber of a home-built stopped-flow injector with dead time of 2 ms.[24] In each injection, 0.35 mL of a solution containing [**1**] (2.5 μM) + TX-100 (0.68 mM) was mixed in with 0.35 mL of pure TX-100 solution ([TX-100] varying from 0 to 30 mM). The signal was monitored at either $\lambda_{em} = 375$ nm or $\lambda_{em} = 480$ nm, with integration and interval times of 1 to 10 ms and a total experiment time ranging from 0.5 to 10 s depending on the decay time. All decay profiles fit well to an exponential form. Experiments were carried out at temperatures of 5.3, 12.6, 19.6, and 24.6 °C. Each experiment was repeated 8 times and the lifetimes of the individual decays from these runs were averaged.

Surface Tension Measurements. Static surface tension measurements on TX-100 solutions were carried out with a DuNöuy tensiometer (DSC 70535) in the laboratory of Prof. E. Kumacheva. The instrument was equipped with a cell that allowed precise temperature control (±1 °C). Measurements were carried out at temperatures of 5.3, 12.6, 19.6, and 24.6 °C. The break in the plot of surface tension vs surfactant concentration is attributed to the critical micelle concentration (cmc).

Dynamic Light Scattering Measurements. Dynamic light scattering measurements were carried out at 90° over a temperature range of 10−50 °C using a variable angle light scattering instrument equipped with an Excel 3000 argon ion laser (1200 mW at 514.5 nm) as the source and a Brookhaven Digital BI 2030AT correlator. The surfactant concentrations were typically 30 × cmc. The autocorrelation functions $g_2(t)$ were analyzed in terms of a continuous distribution of relaxation times τ:

$$g_1(t) = \int_0^\infty \Gamma(\tau) \exp\left(-\frac{t}{\tau}\right) d\tau \qquad (1)$$

where $g_1(t)$ is the normalized electric field autocorrelation function, which is related to $g_2(t)$ through the Siegert relation.[25] $\Gamma(\tau)$ was obtained by regularized inverse Laplace transform (RILT) of the experimental data using a constrained regularization calculation algorithm called REPES without assuming a specific shape.[26] Plots of $\Gamma(\tau)$ vs τ were monomodal and symmetric, with similar full widths at half-height for measurements at the five temperatures examined.

An apparent diffusion coefficient D for a given TX-100 concentration was calculated from the average relaxation times $\langle \tau \rangle$ using $D = (q^2\langle \tau \rangle)^{-1}$, where q is the scattering vector defined as $q = (4\pi n/\lambda) \sin(\theta/2)$, with n the refractive index of the solvent, λ the wavelength of the radiation, and θ the scattering angle. Alternatively, the measured intensity−intensity time correlation function was fitted to a cumulant expansion, eq 4a, where $K_m(\Gamma)$ is the mth cumulant of $g_1(t)$.

$$\ln|g_1(t)| = -\bar{\Gamma}t + \frac{1}{2!}\mu_2 t^2 - \frac{1}{3!}\mu_3 t^3 + \ldots \qquad (2a)$$

$$= K_m(\Gamma)(-t)^m/m! \qquad (2b)$$

In eq 2, $\bar{\Gamma} = \int_0^\infty \Gamma G(\Gamma)\, d\Gamma$, and $\mu_i = \int_0^\infty G(\Gamma)(\Gamma - \bar{\Gamma})^i\, d\Gamma$. In this approach, mutual diffusion coefficients D_1 were calculated from the first cumulant $\bar{\Gamma} = q^2 D_1$. The variance, $\mu_2/\bar{\Gamma}^2$, also provides a measure of the distribution width of $G(\Gamma)$. An apparent hydrodynamic radius

(23) Rharbi, Y.; Kitaev, V.; Winnik, M. A.; Hahn, K. G. *Langmuir* **1999**, *15*, 2259, 2266.

(24) The specifications and a drawing of the stopped-flow injector are provided on our Web site: http://www.chem.utoronto.ca/staff/MAW/mawpage.html.

(25) Berne, B.; Pecora, R. *Dynamic Light Scattering*; Wiley: New York, 1976.

(26) Stepanek, P. In *Dynamic Light Scattering*; Brown, W., Ed.; Oxford University Press: Oxford, 1993; Chapter 4.

Table 1. Influence of Temperature on the cmc, the Aggregation Number of TX-100 Micelles, and the Rate Constant for Pyrene Excimer Formation k_Q in These Micelles

T (°C)	cmc (g/L)	N_{agg}	k_Q (μs^{-1})
5.3	0.29	72	2.87
12.6	0.27	87	3.11
19.6	0.22	102	3.30
24.6	0.19	120	3.67

(R_H) can be obtained from D_1 through the Stokes−Einstein relation:[25] $R_H = k_B T/(6\pi\eta D_1)$, with k_B the Boltzmann constant, T the absolute temperature, and η the viscosity of the solution. For experiments at 10 °C, D_1 values determined from a cumulant analysis of the data for solutions of 2, 4, and 6 g/L were identical to within 5%. At other temperatures, only the 6 g/L solution was examined. Thus at each temperature, the measured D_1 values were assumed to be equal to the "zero concentration" D_0 values.

Micelle Characterization by Fluorescence Decay Measurements. Solutions of **1** in TX-100 (5 g/L and **1**/TX-100 = 0.017) were diluted with the same solution of TX-100 free of **1**. At each temperature, we examined five concentrations of TX-100. The fluorescence decay of these solutions was measured by the single photon timing technique and fitted to the Poisson quenching model.[27] The fitting parameters in this analysis are the intensity at time zero (I_0), the average number of molecules of **1** per micelle ($\langle n\rangle$), and the pseudo-first-order rate constant for excimer formation (k_Q).

$$I(t) = I_0 \exp[t/\tau_0 - \langle n\rangle(1 - \exp(-k_Q t))] \quad (3)$$

The unquenched lifetime τ_0 is known independently from experiments at low [**1**] by fitting these decays to an exponential expression. When the data were fitted to eq 1 with four fitting parameters, the value of the unquenched pyrene lifetime τ_0 was essentially identical with that measured at low probe concentration. The aggregation number N_{agg} is calculated from the dependence of $\langle n\rangle$ on pyrene concentration

$$\langle n\rangle = [\text{pyrene}] \times N_{agg}/([\text{TX-100}] - \text{cmc}) \quad (4)$$

Results

Micelle Characterization. We recently reported time-resolved measurements of excimer formation of **1** in aqueous solutions of TX-100 at room temperature. The fluorescence decay behavior was entirely consistent with a Poisson-distribution model up to a mean occupancy of $\langle n\rangle \approx 3$. Analysis of the fluorescence decay profiles, at surfactant concentrations far above cmc ($c_{TX-100} \geq 10$ cmc), gave a constant aggregation number $N_{agg} = 100$ at room temperature for a large range of surfactant and solute concentrations. This value is consistent with those obtained by light scattering $N_{agg} = 110$ at 25 °C,[28a,b] and fluorescence quenching.[28c] We also reported a relatively low value of the pseudo-first-order excimer formation rate $k_q = 3.7\ \mu s^{-1}$ at room temperature compared to that observed in SDS micelles. Here we extend the characterization of these micelles to other temperatures.

Critical micelle concentrations at each temperature were determined by means of surface tension measurements in an apparatus that allowed for precise temperature control. Cmc values were found to decrease from 0.3 g/L at 5.3 °C to 0.19 g/L at 24.6 °C. The data are collected in Table 1.

In all solutions, at all four temperatures examined here, the time-resolved fluorescence decay behavior was completely consistent with the Poisson-distribution model (eq 1) up to a mean occupancy of $\langle n\rangle \approx 2$. Analysis of the fluorescence decay profiles of these solutions well above the surfactant CMC gave aggregation numbers that were constant for a large range of surfactant and solute concentrations. In Table 1 we show that the mean aggregation number (N_{agg}) increases with temperature from 72 to 120 with an increase in temperature from 5.3 to 24.6 °C. The magnitude of N_{agg} found here at 24.6 °C (120) is significantly higher than that we reported previously (100) at 23 °C. This difference is real and can be attributed to a new batch of Triton X-100 with a slightly different ethylene oxide chain length. A comparison of the two batches of TX-100 will be reported separately.[29] The pseudo-first-order rate constant for excimer formation k_q does not change significantly ($k_Q = 2-4 \times 10^6\ s^{-1}$) over this range of temperatures.

Table 2. Influence of Temperature on the Mutual Diffusion Coefficient D_1, Mean Hydrodynamic Diameter, the Variance $\mu_2/\bar{\Gamma}^2$, and the Diffusion-Controlled Rate Constant for Micelle Collisions

T (°C)	D_1[a] (10^{-7} cm^2/s)	k_{diff}[b] (10^9 M^{-1} s^{-1})	<diameter>[c] (nm)	$\mu_2/\bar{\Gamma}^2$ [a]
10	4.28	4.5	7	0.07
20	5.60	6.3	7.5	0.04
30	5.70	7.9	9.3	0.09
40	5.78	10	11.5	0.09
50	5.81	12	14.3	0.07

[a] From the cumulant analysis of the dynamic light scattering data. [b] Calculated from eq 5. [c] <diameter> = $2R_H$, calculated from D_1.

Hydrodynamic Radii and Diffusion Coefficients of TX-100 Micelles. In Table 2, we report values of the mutual diffusion coefficients (D_1) of TX-100 micelles and their hydrodynamic radii (R_H) in the range of temperatures of 10−25 °C. We use the diffusion coefficient values to calculate the diffusion-controlled collision rate constant k_{diff} in this system,

$$k_{diff} = 4\pi N_A(R_{H1} + R_{H2})\,(D_1 + D_2)/1000 \quad (5)$$

where N_A is Avogadro's number. In this analysis, we assume that D_2 and R_{H2} values for the pyrene-laden micelles are similar to those of the empty micelles (Table 2). The activation energy for this process, calculated from the Arrhenius plot of $\ln(k_{diff})$ vs $1/T$, is found to be 20 kJ/mol.

Exchange Process

Theoretical Considerations. Exchange is monitored by the variation in the fluorescence intensity upon migration of **1** from a micelle bearing more than 2 dye molecules to an empty micelle. Micelles containing more than two molecules of **1** would require multiple exchanges with empty micelles to produce micelles containing a single dye. Although exchange experiments can be carried out for any solution of **1** in TX-100, multiple exchange would complicate the kinetics formalism describing the state of the system during this exchange.[30] In Figure 1 we show how the fraction of micelles $P(n)$ containing n dye molecules varies with the mean occupancy $\langle n\rangle$ for a Poisson distribution of dye molecules among the micelles. Solution with high mean numbers of **1** per micelle (i.e., $\langle n\rangle > 0.5$) would contain a considerable fraction of micelles bearing 1, 2, 3, and even 4 dye molecules. Simplifying the experimental analysis requires the selection of solutions with a mean occupancy number of **1** per micelle in the range $0.2 < \langle n\rangle \leq 0.5$. These solutions contain mainly micelles bearing 0, 1, or 2 molecules of **1**. Those containing 3 or more molecules of dye can be safely neglected.

(27) Maestri, M.; Infelta, P.; Grätzel, M. *J. Chem. Phys.* **1978**, *69*, 1522.
(28) (a) Streletzky, K.; Phillies, G. D. J. *Langmuir* **1995**, *11*, 42−47. (b) Brown W., Rymden R.; van Stam J.; Almgren M.; Svensk G. *J. Phys. Chem.* **1989**, *93*, 2512−2519. (c) Alargova R. G.; Kochijashky, I. I.; Sierra, M. L.; Zana R. *Langmiur* **1998**, *14*, 5412−5418.
(29) Li, M.; Rharbi, Y.; Winnik, M. A. Manuscript in preparation.
(30) Barzykin, A. V.; Tachiya, M. *J. Phys. Chem.* **1994**, *98*, 2677.

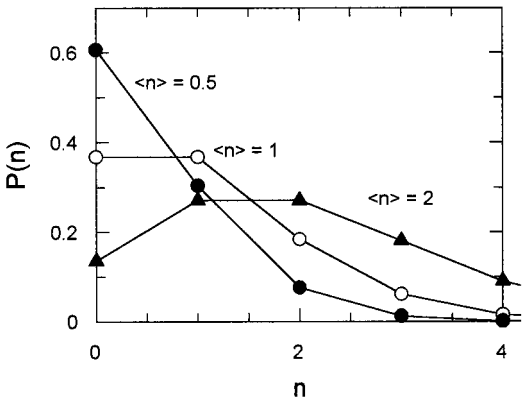

Figure 1. Plot of the calculated fraction of micelle $P(n)$ bearing n solute molecules distributed as Poisson, for various mean occupancy numbers $\langle n \rangle = 0.5$, 1, and 2.

In our earlier report,[21] we showed, based upon previous calculations by Zana[2] and by Infelta,[31] that the fluorescence quantum yield for excimer emission Φ_E, compared to the fluorescence quantum yield for excimer itself Φ^0_E, is described by eq 6a.[32] The relative quantum yield for monomer fluorescence Φ_M compared to that of the unquenched monomer Φ^0_M is given by eq 6b.

$$\Phi_E/\Phi^0_E = \tau^\circ k_Q(n-1)/(\tau^\circ k_Q(n-1)+1) \qquad (6a)$$

$$\Phi_M/\Phi^0_M = 1/(\tau^\circ k_Q(n-1)+1) \qquad (6b)$$

In the simple case of a system containing micelles with only 0, 1, and 2 molecules of **1**, the measured excimer (I_E) and monomer (I_M) fluorescence intensities become linearly dependent on the fraction of micelles $P(t)$ containing a pair of molecules of **1** at time t.

$$I_E \propto \Phi_E/\Phi^0_E = \Phi_E/\Phi^0_E(0) - \tau^\circ k_Q/(\tau^\circ k_Q + 1)\,[P(0) - P(t)] \qquad (7)$$

$$I_M \propto \Phi_M/\Phi^0_M = \Phi_M/\Phi^0_M(0) + (2\tau^\circ k_Q + 1)/(\tau^\circ k_Q + 1)[P(0) - P(t)] \qquad (8)$$

Exchange Experiments. In Figure 2, we present the fluorescence spectrum of a solution of **1** in water at a bulk concentration of 2.15 μM in the presence of 0.68 mM TX-100. This spectrum, labeled "Prior", has a broad excimer emission with a peak at 480 nm, in addition to the monomer fluorescence with a (0,0) band at 375 nm. Upon pulsed excitation of this solution, the pyrene decay fits to the Poisson distribution model with a mean occupancy number $\langle n \rangle = 0.44$ and $k_q = 2.4\ \mu s^{-1}$. When an aliquot of a concentrated TX-100 solution is mixed with this solution, to bring the total TX-100 concentration to 5.89 mM, the spectrum evolves to that labeled "After exchange". This spectrum has a strong monomer emission, but no discernible excimer band. Consistent with the absence of excimer, we find that the pyrene decay of **1** in the solution after exchange exhibits an exponential decay with a lifetime of 174 ns.

In Figure 3a, we show the results of two time-scan experiments in which we monitor the decrease in excimer emission intensity (I_E, 480 nm) and the increase in monomer emission intensity (I_M, 375 nm) following the rapid addition of excess TX-100 surfactant to the solution with $\langle n \rangle = 0.44$. Both the decease in I_E and the growth in I_M fit to an exponential expression with comparable exchange rates, k_{obs}. The goodness of these fits is confirmed by the random distribution of the residuals (Figure 3b), but with a higher signal-to-noise ratio in the I_E decay (where the noise is ca. 1% of the signal intensity) than in I_M (10% of the signal intensity). From different runs on the same sample, the magnitude of exchange rate is reproducible to within less than 10% when it is calculated from I_E data and

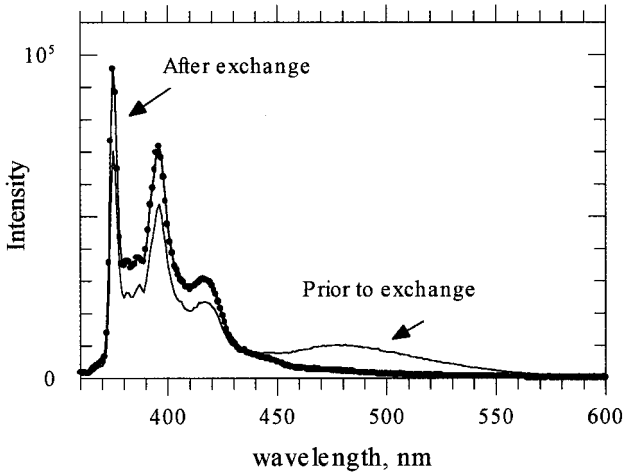

Figure 2. Emission spectra ($\lambda_{ex} = 346$ nm) of **1** solubilized in aqueous solutions of TX-100 micelles. In the spectrum labeled "Prior to exchange", [**1**] = 2.15 μM and [TX-100] = 0.68 mM. The spectrum "After exchange" refers to the solution obtained by mixing the original solution with an equal volume of TX-100 solution to raise the surfactant concentration to [TX-100] = 5.89 mM.

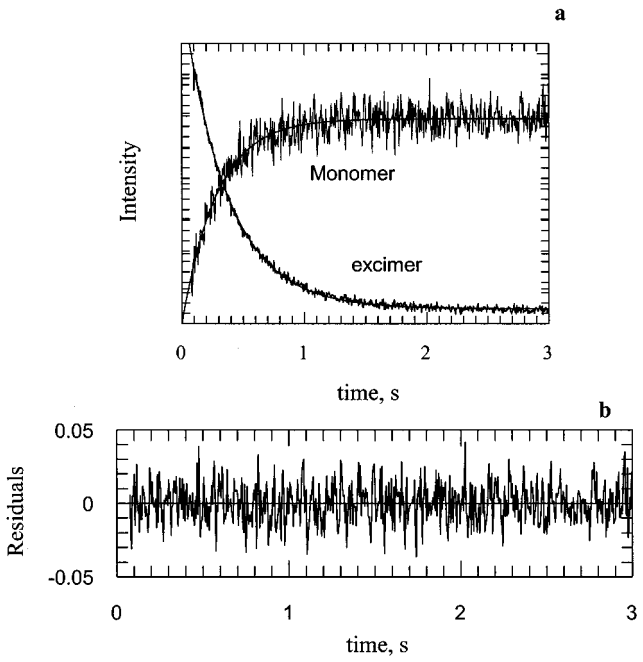

Figure 3. (a) Time-scan experiments monitoring the increase in the monomer emission I_M ($\lambda_{em} = 375$ nm) and the decrease in the excimer emission I_E ($\lambda_{em} = 480$ nm) after stopped-flow mixing of a solution of **1** in TX-100 micelles ([**1**] = 2.15 μM, [TX-100] = 0.68 mM) with an equal volume of TX-100 solution ([TX-100] = 7.7 mM) at temperature of 5.3 °C. The solid lines represent the exponential curves which best fit the data. (b) Residuals from the best fit of the excimer data to an exponential curve.

(31) Infelta, P. P.; Grätzel, M. *J. Chem. Phys.* **1979**, *70*, 179.

(32) The term Φ^0_E is defined in such a way that it represents the hypothetical quantum efficiency of excimer emission if the excimer could be formed with unit efficiency; cf.: Birks, J. B. *Photophysics of Aromatic Molecules*; Wiley-Interscience: New York, 1971.

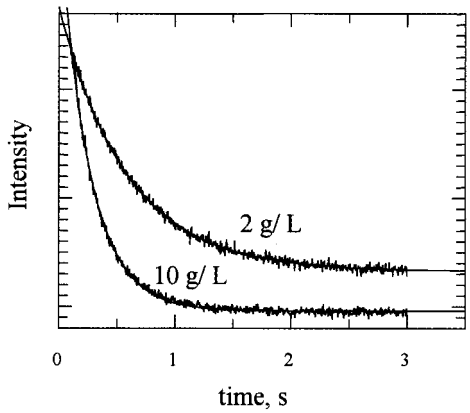

Figure 4. Time-scan experiments monitoring the decrease in I_E after mixing of a solution of **1** in TX-100 micelles ([**1**] = 2.15 μM, [TX-100] = 0.68 mM) with an equal volume of TX-100 solutions at concentrations of 3 (2 g/L) and 15.4 mM (10 g/L) at a temperature of 5.3 °C.

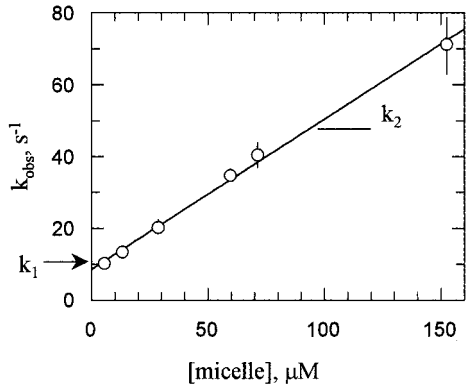

Figure 5. The relaxation rates k_{obs} calculated from the fits of the data from individual stopped-flow experiments plotted vs the concentration of empty TX-100 micelles. These decays were monitored at λ_{em} = 480 nm with λ_{ex} = 346 nm. The error bars refer to one standard deviation in repeated measurements at each empty micelle concentration.

reproducible to within 30% when calculated from I_M. In the discussion below, we will consider only k_{obs} values calculated from the excimer decay.

When the kinetics experiments are repeated at different TX-100 concentrations, we notice a strong dependence of the exchange rate on the concentration of unoccupied micelles (Figure 4). The relaxation rate k_{obs} calculated from the fits of the individual decays at 19.6 °C varies between 6 and 60 s^{-1}. An important observation is that the exchange rate observed here is more than 10^4 times slower than the reported exit rate of TX-100 molecules from the micelles at similar temperatures ($k^- = 1.1 \times 10^6$ s^{-1}).[5] Even though the individual surfactant molecules are in a state of rapid exchange, the triglyceride molecules **1** remain inside the individual micelles.

In Figure 5 we plot values of k_{obs} vs [micelle]. In these plots, the k_{obs} values are calculated from the decay of I_E, and the values calculated for the micelle concentration take account of the temperature dependence of the cmc and of the mean aggregation number. Here we can identify two main characteristics of the data plotted in Figure 4: (1) the linear dependence of k_{obs} on the concentration of empty micelles ([micelles]), and (2) the nonzero intercept k_1. It is clear from these plots that the exchange mechanism described by k_{obs} consists of two competing processes: a second-order process with linear dependence of k_{obs} on [micelles], and a first-order process with a rate independent of the empty micelle concentration.

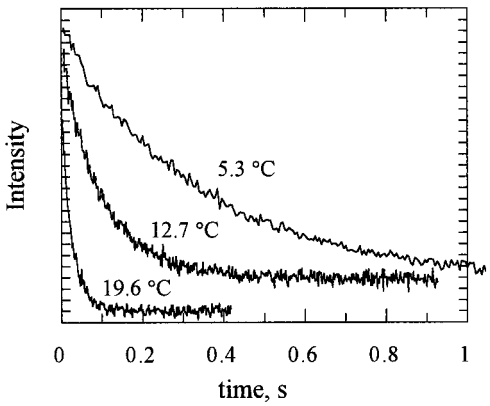

Figure 6. Time-scan experiments monitoring the decrease in I_E at temperatures of 5.3, 12.6, and 19.6 °C following stopped-flow mixing of a solution of **1** in TX-100 micelles ([**1**] = 2.15 μM, [TX-100] = 0.68 mM) with an equal volume of TX-100 solutions ([TX-100] = 7.36 mM). The solid lines represent the best exponential fits to the data.

Temperature Dependence of the Exchange Processes. In Figure 6, we show time-scans following rapid mixing of empty and solute-bearing micelles at temperatures of 5.3, 12.6, and 19.6 °C. Although there is a strong dependence of the exchange kinetics on the temperature, our decays fit to single-exponential profiles for all temperatures investigated. The relaxation rates (k_{obs}) calculated from the best fits of the individual decays, as observed above, show a linear dependence on [micelles] and a finite intercept (Figure 7, parts a and b). Both the slopes of the plots and the magnitudes of the intercepts in Figure 7 increase with increasing temperature The best-fit values of k_2 and k_1 at each temperature are collected in Table 3. Arrhenius plots of k_2 and k_1 are linear (Figure 8) with activation energies of 160 kJ/mol for k_2 and 100 kJ/mol for k_1.

Discussion

As mentioned in the Introduction, one can identify three distinct mechanisms for surfactant or solute exchange among micelles. Chart 2 in the Introduction illustrates these three mechanisms for exchange of solutes between spherical aqueous micelles. The first mechanism (exchange via water) involves the exit of the solute from the micelle into the water phase and its re-entry in an empty micelle. This process exhibits first-order kinetics because exit of the solute is the rate-limiting step. The rate of this step is described by the first-order rate constant k_{exit}. The second mechanism (collision−exchange−separation) involves interaction of the solute-containing micelle with an empty micelle in the rate-limiting step, or prior to the rate-limiting step. This mechanism is characterized by second-order kinetics. The third mechanism (fragmentation−growth) involves break-up of the normal-size solute-bearing micelle into two sub-micelles each containing a single solute, followed by growth of these sub-micelles either by fusion with empty micelles or by interaction with surfactant monomers. The fragmentation step is rate limiting, and the rate of this process is described by the first-order rate constant k_{fr}.

In any individual experiment, exchange could occur simultaneously by all three mechanisms. Under our experimental conditions of low $\langle n \rangle$ values and a large excess of empty micelles, $P(t)$, the fraction of micelles bearing a pair of **1** at time t, would decrease exponentially in time with a first-order rate constant k_{obs}.

$$I_E \propto P(t) = P(0) \exp(-k_{obs}t) \qquad (9)$$

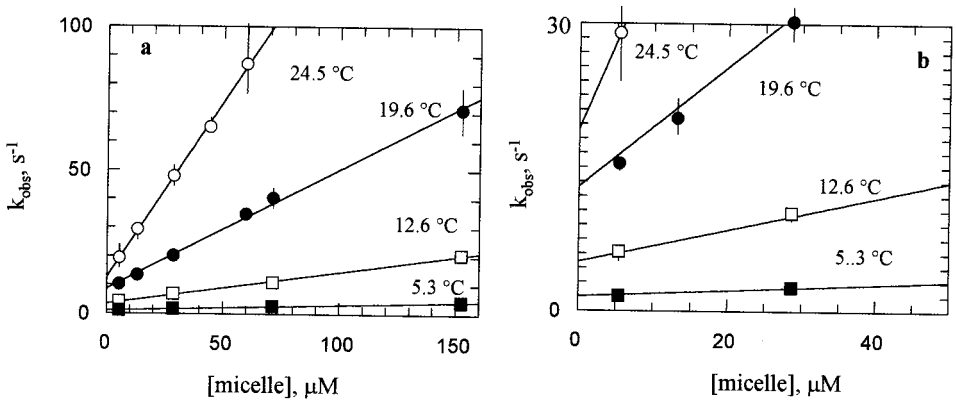

Figure 7. (a) The relaxation rates k_{obs} calculated from the fits of the data from individual stopped-flow experiments plotted vs the concentration of TX-100 micelles for temperatures of 5.3, 12.6, 19.6, and 24.6 °C. The error bars refer to one standard deviation for repeated measurements at each empty micelle concentration. (b) Another representation of the data in part a, emphasizing the limit of [micelle] approaching 0.

Table 3. Effect of Ttemperature on the First- and Second-Order Rates for Exchange of the Probe **1** in Triton X-100 Micelles

T (°C)	$10^{-6}\,k_2$ ($M^{-1}\,s^{-1}$)	k_1 (s^{-1})
5.3	0.015	1.0
12.6	0.098	3.4
19.6	0.425	8.6
24.6	1.47	12.6

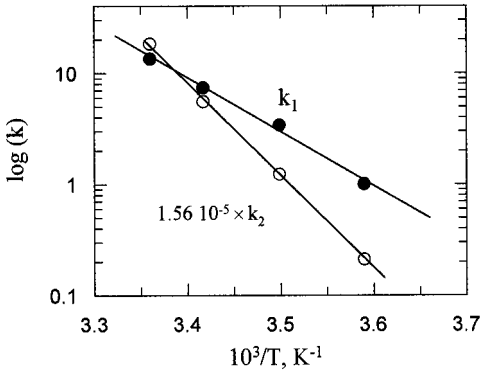

Figure 8. Arrhenius plot of the second-order rate constant k_2 and the first-order rate constant k_1 vs $1/T$.

The collision−exchange−separation mechanism is characterized by bimolecular kinetics with a rate proportional to k_2[micelle]. In the simple case of low $\langle n \rangle$ values and excess unoccupied micelles, the concentration of empty micelles remains essentially unchanged during a stopped-flow experiment. Under these conditions, k_{obs} is the pseudo-first-order rate which contains contributions both the first-order and second-order exchange processes.

$$k_{obs} = k_1 + k_2[\text{micelle}] = k_1 + k_2([\text{TX-100}] - \text{cmc})/N_{agg} \quad (10a)$$

$$k_1 = k_{exit} + k_{fr} \quad (10b)$$

If the process described by k_{exit} is unimportant because of the insolubility of **1** in water, the other two processes can be separated because they exhibit different kinetics.

The Second-Order Process. Except at very low surfactant concentration, the most important pathway for solute exchange for TX-100 micelles is the second-order process (collision−exchange−separation) shown in Chart 2. This process must involve a number of intermediates. We imagine four discrete steps: (1) collision of a solute-containing micelle with an empty micelle, (2) formation of an aggregate consisting of the two micelles, (3) exchange of **1** within this aggregate, and (4) separation of the aggregate into two micelles of normal size. It is relatively straightforward to show that the micelle collision step itself is not rate limiting. This conclusion can be reached by comparison of the magnitude of k_2 to the diffusion-controlled rate constant k_{diff} calculated from eq 3. Although the measured rate of exchange is relatively rapid ($k_2 = 1.47 \times 10^6\ M^{-1}\ s^{-1}$ at 24.6 °C), it is still more than 5000 times slower than the diffusion-controlled rate at the same temperature $k_{diff} = 7 \times 10^9\ M^{-1}\ s^{-1}$. This conclusion is reinforced by the temperature dependence of the two second-order rate constants. In Figure 9 we present Arrhenius plots of k_2 and k_{diff}. The activation energy for the exchange of **1** is found to be 160 kJ/mol, which is 8 times greater than the activation energy for the diffusion-controlled mechanism, 20 kJ/mol.

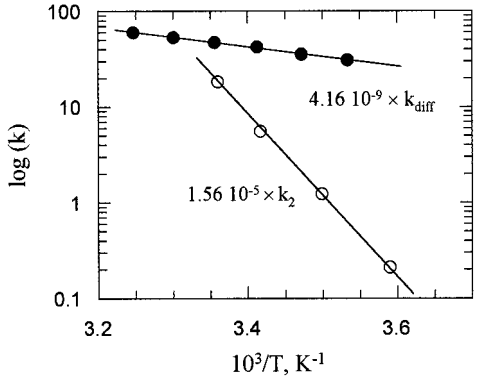

Figure 9. Arrhenius plots of the second-order rate constant k_2 calculated from the dependence of k_{obs} vs [micelle] and the diffusion-controlled rate constant k_{diff} calculated from eq 3.

Chart 3

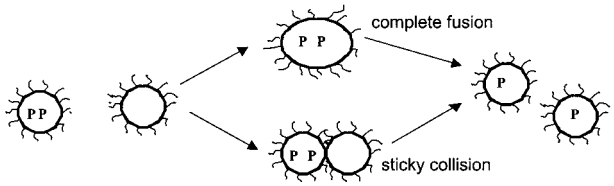

There is agreement in the literature[7] that the collision−exchange−separation mechanism involves the formation of an intermediate aggregate with a short but finite lifetime, in which dye and surfactant exchange. However, there is no agreement on its nature. Chart 3 shows two possible mechanisms of dye migration between collided micelles. One involves fusion of two micelles to form a super-micelle with a hydrophobic core

in which the solutes move freely. The alternative process involves adhesion (a sticky collision) of two micelles for a short time synchronized with exchange of **1** by permeation through the layer consisting of the micellar headgroups. These two mechanisms are kinetically identical but the factors that contribute to the energy barriers are different. The 160 kJ/mol activation barrier determined above might represent the barrier to exchange in the sticky micelle dimer or it may represent the barrier to fusion to form a super-micelle.

The Fusion Mechanism. In terms of this model, two normal size micelles collide and fuse together to form a super-micelle containing $2 \times N_{agg}$ surfactant molecules followed by dye diffusion inside its core. The super-micelle then undergoes fission to form two normal size micelles each bearing a single dye. We can cite at least four contributions to the barrier for exchange via this mechanism, with three dependent on the micelle−micelle interaction and one dependent on the proprieties of the solute. The first contribution is the steric interaction of the poly(ethylene oxide) stabilizer chains, which provide both an entropic and a hydration barrier to close approach of the micelle cores. The second involves the energy changes within the aggregate to accommodate $2 \times N_{agg}$ surfactant monomer in the super-micelle. The third contribution is the activation energy associated with rearrangement of the surfactant molecules accompanying fusion of the two micelles. The fourth contribution is the barrier to diffusion of the solute inside the core.

It is possible to argue that, for TX-100 micelles, core fluidity does not play an important role in limiting the exchange kinetics. A measure of the micelle core fluidity is provided by the rate of excimer formation between two molecules of **1** solubilized in a TX-100 micelle. The first-order rate constant for this process (k_Q) is obtained as a fitting parameter in the fluorescence decay analysis of solutions of **1** in TX-100. These values are constant over a wide range of surfactant and solute concentrations and vary from 2×10^6 to 4×10^6 s^{-1} between 5 and 25 °C. Thus the micelle core acts as a fluid droplet on the time scale of milliseconds, and is unlikely to act as a barrier to the fusion process.

A balance of interactions determines micelle size and shape at equilibrium.[33] Phase separation creates a surface energy, which is minimized by the formation of large micelles: the larger the micelles, the smaller the total surface area in the solution. The decrease in surface area is opposed by the need to accommodate at the micelle surface the headgroups of each surfactant. Combining two micelles into a super-micelle will result in a decrease in surface energy but an even larger increase in headgroup repulsion as the headgroups are constrained to an area smaller than the optimum value. The increase in energy necessary to accommodate $2 \times N_{agg}$ surfactant molecules in the super-micelle is expected to be reflected by the micellar polydispersity. The higher the polydispersity, the lower this contribution is to the energy barrier, since super-micelles and sub-micelles can coexist in a thermodynamic equilibrium with the normal size micelles as a result of the polydispersity. Some authors have found, particularly for nonionic micelles, that the increase in the aggregation number with increasing temperature is accompanied by a strong increase in the micelle polydispersity.[34,35] We found that the aggregation number of TX-100 micelles increased from 75 to 120 (Table 1) between 5.3 and 24.6 °C. Our dynamic light scattering experiments indicate that no major change in micelle polydispersity occurs over this temperature range.

The Sticky-Collision Mechanism. This mechanism involves the collision of two micelles followed by their adhesion for a short time, during which the exchange of **1** takes place. This process involves passage of the solute through the ethylene oxide layer between the micelles, perhaps assisted and accompanied by a small number of surfactant molecules. This type of mechanism was inferred by Cabane et al. from their studies of Ostwald ripening in alkane−water−nonionic surfactant microemulsions.[17a] The energy barrier to the exchange in this mechanism will have contributions from the factors that affect the adhesion ability of these micelles combined with the solubility of the solute in the polymer constituting the protective corona. One imagines that in the transfer step, hydrophobic molecules will exchange more slowly than hydrophilic ones.

Comparison of These Models. Zana and Weill[19] studied the exchange of pyrene between TX-100 micelles by following the kinetics of excimer formation through fluorescence decay measurements. They analyzed their decays using a modified Poisson quenching model by taking into consideration the exchange of pyrene molecules during their excited state. They inferred that, for a wide range of temperatures, the fusion−fragmentation process takes place, with a second-order rate constant of $k_2 \cong 5 \times 10^8$ M^{-1} s^{-1} at 25 °C. This value is 300 times higher than that found in our experiments. At first glance, one might attribute the substantial difference in rate constants to the difference in dyes employed in the two experiments. One might then infer that exchange occurs by the sticky collision mechanism, since the rate of the fusion mechanism should be independent of the type of dye. Of course, one might also argue that in the fluorescence decay measurements, the exchange rate is obtained by fitting an additional parameter to an already complex expression. Some other process that occurs on the time scale of 100 ns to a few microseconds may be involved in the excimer kinetics. In the stopped-flow experiments, exchange is measured directly, but there is no sensitivity to processes that occur in less than 10 ms.

To test these ideas, one should repeat the stopped-flow experiments on TX-100 micelles with different pyrene derivatives characterized by different water solubilities, *X*. Huang in our laboratory recently prepared samples of 1-octylpyrene (C_8-Py) and 1-dodecylpyrene (C_{12}-Py). While detailed experiments with these probes are still in progress,[36] we show the results of stopped-flow experiments in Figure 10, which examine the probe dependence of the exchange rate for TX-100 micelles. In Figure 10 we plot values of k_{obs} vs [micelle] for C_8-Py, C_{12}-Py, and **1**. What is remarkable about these plots is that they are all linear with virtually identical slopes. The intercepts increase as the size of alkyl chains decreases. The fact that the plots are parallel indicates that the rate of the second-order exchange is independent of the solute, which provides strong support for a fusion mechanism as the second-order exchange process in TX-100 micelles. We conclude that fusion is rate limiting, and that the second-order rate constant k_2 obtained from our experiments is equal to the rate constant k_{fus} describing the micelle fusion rate.

The First-Order Process. The intercepts in Figure 7 describe an exchange process for **1** in TX-100 micelles characterized by a first-order kinetics. Values of k_1 vary from 1 s^{-1} at 5.3 °C to 12.6 s^{-1} at 24.6 °C. In the discussion above, we assumed that the solubility of **1** in water was so low that this rate constant could not describe the exit rate of **1** from the micelles. To test

(33) Israelachvili, J. *Intermolecular and Surface Forces*; Academic Press: London, 1992; Chapter 17.

(34) Corkill, J.; Goodman, J.; Walker, T.; Wyer, J. *Proc. R. Soc. London, Ser. A* **1969**, *312*, 243.

(35) Mazer, N.; Benedek, G.; Carey, M. *J. Phys. Chem.* **1976**, *80*, 1075.

(36) Huang, X.; Rharbi, Y.; Winnik, M. A. To be submitted for publication.

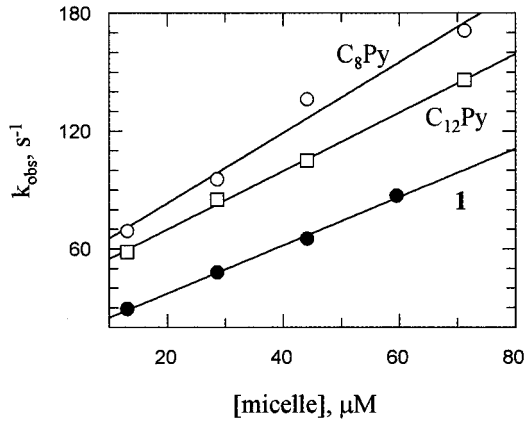

Figure 10. The relaxation rates k_{obs} vs the concentration of empty TX-100 micelles for exchange experiments using various pyrene derivatives 1-octylpyrene, 1-dodecylpyrene, and **1**. These decays were monitored at $\lambda_{em} = 480$ nm with $\lambda_{ex} = 346$ nm.

this idea, we make a much less stringent assumption: We imagine that the exit rate of **1** from the micelle phase into the water phase should occur at similar rates for different micelles. We prepared solutions of **1** in SDS micelles that exhibited significant excimer emission. In the absence of added salt, the exchange of **1** among SDS micelles is too slow to be detected. These experiments, and the influence of salt on the exchange rate, will be described in detail in a separate report.[37] Our results are in accord with the fragmentation−growth model of micelle exchange.

In the fragmentation−growth mechanism, micelles bearing two molecules of **1** break down into two sub-micelles, each containing a single dye molecule. These sub-micelles can grow either by association with surfactant monomers or by fusion with other sub-micelles. The rate of this process increases with temperature (Figure 8 and Table 3), and is characterized by an activation energy of 100 kJ/mol. We see that the fragmentation step of the first-order exchange mechanism has a smaller activation energy, but a smaller preexponential factor, than the fusion step of the second-order process. Here we have the unusual situation of a first-order process favored by activation energy but disfavored by entropy compared to a second-order process. To understand this result, one has to recognize that in terms of thermodynamics, micellization of typical nonionic surfactants, including Triton X-100, is endothermic.[38] For these surfactants, the formation of micelles is favored by entropy, presumably associated with randomization of the water surrounding the hydrophobes as they move from solution in water into the core of the micelle. To explain our findings, we imagine that fragmentation of a normal micelle into two solute-bearing sub-micelles must be accompanied by an exothermic contribution from reorganization of the surfactant and solute into the sub-micelles, as well as an important decrease in entropy.

The increase in temperature from 5.3 to 24.6 °C is also accompanied by an increase in the aggregation number from 72 to 120. A number of experiments reported in the literature have been interpreted as indicating that an increase in micelle aggregation number is accompanied by a significant increase in the micelle polydispersity.[29,30] The fragmentation−growth model is consistent with this idea, since sub-micelles and super-

Chart 4

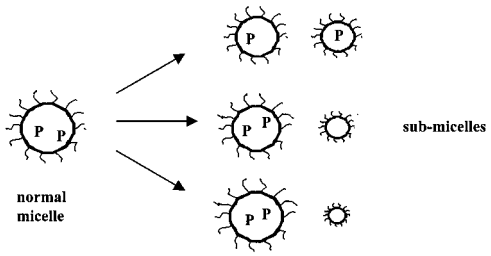

micelles coexist in thermodynamic equilibrium with the normal size micelles, and the population of these small and large micelles increases as the polydispersity increases. For example, Malliaris et al.[18] have inferred a similar mechanism from their studies of pyrene exchange between dodecylammonium chloride micelles at different salt concentrations. They concluded that the rate of the fragmentation−association process is accentuated by the increase in micelle polydispersity as a result of increased the salt concentration. A recent paper by Hall,[39] however, takes issue with this, and suggests that the size polydispersity remains narrow. He shows that one can account for all of the experimental evidence about the influence of salt on SDS micelles in a more coherent way without invoking a broadening of the micelle polydispersity. Our dynamic light scattering data, Table 3, are inconsistent with any substantial change in TX-100 micelle polydispersity between 5.3 and 24.6 °C.

In Figure 10, we observe that the rate of the first-order process is sensitive to the structure of the probe, with $k_1(\mathbf{1}) < k_1(C_{12}\text{-Py}) < k_1(C_8\text{-Py})$. There are in principle two explanations for this result. The first is that for the smaller two probes, the exit−reentry mechanism (eq 10b) plays a role and increases the exchange rate. The second is that the fragmentation−growth mechanism operates for all three probes, but the rate of this process depends on the solute. We have preliminary evidence to favor the second explanation: We find that in the absence of added salt the first-order exchange rates of C_{12}-Py and C_8-Py are much slower in SDS micelles than those found for TX-100 micelles. If the rate of exit of a solute from a micelle is not very dependent on the type of micelle, then the exchange process of our three probes among TX-100 micelles is surfactant assisted. The differences we find in the first-order exchange rates indicate that the extent of surfactant assistance needed for exchange by this route depends on the probe.

The conclusions of the preceding paragraph are very important for developing a model that allows one to recognize the difference between solute exchange experiments and probe-free measures of micelle relaxation. In traditional relaxation measurements, such as pressure-jump and temperature-jump experiments, one senses the entire spectrum of relaxation processes of the micelles in the system. The fragmentation−growth contribution to surfactant exchange involves all possible combinations of fragmentation steps. A normal micelle containing g surfactant monomers (N_g) can fragment into micelles and sub-micelles containing $i + j = g$ monomers. These steps are illustrated in Chart 4 and described by eq 11, where we exclude $i,j = 1$ to separate exchange via exit of individual surfactant monomers from fragmentation.

$$N_g \rightarrow N_i + N_j \qquad (i \le j \le g/2;\ i + j = g;\ i,j \ne 1) \quad (11)$$

In our model, a sub-micelle must contain a minimum number of surfactant molecules to solubilize a water-insoluble probe.

(37) Rharbi, Y.; Winnik, M. A. Manuscript in preparation.

(38) (a) Andersson, B.; Olofsson, G. *J. Chem. Soc., Faraday Trans. 1* **1988**, *84*, 4087. (b) Winnik, M. A.; Bystryak, S. M.; Odrobina, E. *Langmuir*. Submitted for publication.

(39) Hall, D. G. *Langmuir* **1999**, *15*, 3483.

The number of surfactant molecules required will depend on the size of the probe and perhaps the presence of polar groups in the probe that can form hydrogen bonds with water molecules. In Chart 2 we suggest that of the three fragmentation pathways illustrated, only the step that gives relatively large sub-micelles, with the size of both fragments not too different from $g/2$, is effective at repartitioning the probe. In the other fragmentation steps, one of the sub-micelles is too small to solubilize **1** effectively.

As a final comment, we note that one expects the fragmentation rate of super-micelles will be much faster than that of normal micelles. Super-micelles have a much higher free energy than normal micelles. We expect that the transition state for fission of a super-micelle into two normal micelles will benefit from the energy release along the path toward formation of two more stable entities. Thus there is no reason to expect fragmentation of the super-micelle would be as slow as the k_1 value for **1** determined from the intercept in Figure 10. In the fusion−fragmentation mechanism, we believe that the fusion step is rate limiting.

Acknowledgment. The authors thank ICI, ICI Canada, and NSERC Canada for their support of this research. The authors would also like to thank Dr. R. Zana (France), Professors B. Cabane (France) and Dr. C. Bohne (Canada) for their valuable comments, and Dr. X. Huang for samples of octylpyrene and dodecylpyrene.

JA9942585